

**High-pressure EXAFS study of vitreous GeO<sub>2</sub> up to 44 GPa**M. Baldini,<sup>1,2,\*</sup> G. Aquilanti,<sup>3,4</sup> H.-k. Mao,<sup>5,6,7</sup> W. Yang,<sup>6,7</sup> G. Shen,<sup>6,7</sup> S. Pascarelli,<sup>3</sup> and W. L. Mao<sup>1,2,8</sup><sup>1</sup>*Geological and Environmental Sciences, Stanford University, Stanford, California 94305, USA*<sup>2</sup>*Stanford Institute for Materials and Energy Science, SLAC National Accelerator Laboratory, Menlo Park, California 94025, USA*<sup>3</sup>*European Synchrotron Radiation Facility, BP 220, F-38043 Grenoble, France*<sup>4</sup>*Sincrotrone Trieste, Area Science Park s.s.14 Km. 163.5, Basovizza, Trieste 34149, Italy*<sup>5</sup>*Geophysical Laboratory, Carnegie Institution of Washington, Washington, DC 20015, USA*<sup>6</sup>*HPCAT, Carnegie Institution of Washington, Argonne, Illinois 60439, USA*<sup>7</sup>*HPSynC, Carnegie Institution of Washington, Argonne, Illinois 60439, USA*<sup>8</sup>*Photon Science, SLAC National Accelerator Laboratory, Menlo Park, California 94025, USA*

(Received 16 September 2009; revised manuscript received 6 November 2009; published 4 January 2010)

High-pressure extended x-ray absorption fine-structure measurements were performed on amorphous GeO<sub>2</sub> over increasing and decreasing pressure cycles at pressures up to 44 GPa. Several structural models based on crystalline phases with fourfold, fivefold, and sixfold coordination were used to fit the Ge-O first shell. The Ge-O bond lengths gradually increased up to 30 GPa. Three different pressure regimes were identified in the pressure evolution of the Ge-O bond distances. Below 13 GPa, the local structure was well described by a fourfold “quartzlike” model whereas a disordered region formed by a mixture of four- and five-coordinated germanium-centered polyhedra was observed in the intermediate pressure range between 13 and 30 GPa. Above 30 GPa the structural transition to the maximum coordination could be considered complete. The present results shed light on the GeO<sub>2</sub> densification process and on the nature of the amorphous-amorphous transition, suggesting that the transition is more gradual and continuous than what has been previously reported.

DOI: [10.1103/PhysRevB.81.024201](https://doi.org/10.1103/PhysRevB.81.024201)

PACS number(s): 62.50.-p, 07.35.+k, 81.05.Kf, 87.64.kd

**I. INTRODUCTION**

GeO<sub>2</sub> is a group-VI oxide whose properties are of interest to fundamental physics and chemistry as well as in applied fields such as materials science. Studies of the behavior of crystalline, amorphous, and liquid GeO<sub>2</sub> have also been motivated in part due to its being an analog to SiO<sub>2</sub>.<sup>1</sup> The discovery of a pressure-driven amorphous-amorphous transition in GeO<sub>2</sub> is of significant importance for glass theory, and the resulting debate on the nature of this transition has enhanced interest in the pressure-dependent behavior of this amorphous compound.<sup>2-5</sup>

During the past two decades, the pressure and temperature phase diagram of crystalline GeO<sub>2</sub> has been elucidated.<sup>6</sup> At ambient temperature and pressure the crystalline compound has two polymorphic forms: the  $\alpha$ -GeO<sub>2</sub> phase with an  $\alpha$ -quartzlike structure ( $P3_221$ ) (Ref. 7) and the  $r$ -GeO<sub>2</sub> phase with a rutile structure ( $P4_2/mnm$ ).<sup>8</sup> The  $\alpha$ -GeO<sub>2</sub> phase is characterized by a GeO<sub>4</sub> tetrahedral framework in which a germanium atom is surrounded by four oxygen atoms. The  $r$ -GeO<sub>2</sub> phase contains GeO<sub>6</sub> octahedra. The first evidence of a pressure-induced coordination change from fourfold to sixfold around the Ge atom was observed in crystalline  $\alpha$ -GeO<sub>2</sub> between 7 and 9 GPa.<sup>9</sup> A structural phase transition to a poorly crystalline monoclinic  $P2_1/c$  phase occurred simultaneously and was found to be metastable from ambient pressure up to at least 50 GPa at room temperature.<sup>10-12</sup> The crystalline sample also showed complex behavior at high pressure and temperature where several additional structural transformations were observed.<sup>13-15</sup>

A pressure-induced amorphous-amorphous transition from fourfold to sixfold coordination was observed by Itie *et*

*al.* in 1989 (Ref. 9) and the possibility of a first-order transition in amorphous GeO<sub>2</sub> was suggested.<sup>16</sup> The details of the local structure changes still require clarification, and the mechanism of the transition—whether it is a continuous process with an intermediate state or an abrupt collapse into sixfold GeO coordination—is still a matter of debate. At ambient pressure the structure of GeO<sub>2</sub> glass is dominated by tetrahedral units much like  $\alpha$ -GeO<sub>2</sub>.<sup>17</sup> The pressure evolution of the local structure of amorphous GeO<sub>2</sub> has been studied by extended x-ray absorption fine structure (EXAFS) up to 29 GPa.<sup>9</sup> The major transformation occurs between 6 and 8 GPa where the high-pressure Ge-O bond lengths appear to be similar to those expected for sixfold coordination and thus the rutile form.<sup>9</sup> The appearance of a two domain region, characterized by the coexistence of both GeO<sub>4</sub> and GeO<sub>6</sub> units, is suggested by the pressure evolution of the Ge-O distance between 6 and 10 GPa and is supported by high-pressure Raman measurements<sup>18</sup> and thermodynamic experiments.<sup>19</sup> High-pressure x-ray and neutron-diffraction experiments have been performed at pressures up to 15 and 5 GPa, respectively, by Guthrie *et al.*<sup>20</sup> They reported a pure fivefold-coordinated structure in the intermediate pressure range between 6 and 10 GPa, and a fully sixfold-coordinated glass at 15 GPa. Density, x-ray diffraction, and Raman measurements were performed up to 35 GPa (Ref. 21) confirming the completion of the coordination change above 13 GPa and suggesting a steplike evolution in the pressure range between 2 and 13 GPa.<sup>21</sup> In contrast, recent EXAFS investigations of both crystalline and amorphous GeO<sub>2</sub> have shown that the fourfold to sixfold transformation is continuous and not complete until at least 13 GPa.<sup>22</sup> Finally, GeO<sub>2</sub> glass shows different thermal behavior depending on whether its

coordination is fourfold, sixfold, or an intermediate coordinated form.<sup>23</sup>

Molecular-dynamics calculations have also been performed to investigate the high-pressure behavior of amorphous GeO<sub>2</sub>. Micoulaut reported Ge-O bond distances up to 30 GPa, finding a stepwise change in the local structure around 9 GPa and then a continuous evolution of the Ge-O bond distances beyond that.<sup>6</sup> A fully sixfold-coordinated state was not observed even at 30 GPa.<sup>24</sup> Shanavas *et al.*<sup>25</sup> reported a gradual increase in Ge-O bond lengths between 0 and 10 GPa, and a constant evolution of Ge-O bond distances with pressure above 10 GPa, in qualitative agreement with previous experimental results.<sup>9</sup> The state does not appear to be fully sixfold coordinated even at pressures as high as 30 GPa and a monotonic increase in coordination number was observed over the entire pressure range. This suggests the coexistence of four- and six-coordinated Ge atoms, rather than the formation of a purely fivefold-coordinated state.<sup>25</sup> More recent calculations have shown that, although coordination increases steadily with pressure, the number of oxygen atoms around a Ge atom gradually reaches sixfold coordination.<sup>26</sup> The coexistence of four-, five-, and six-coordinated Ge atoms and the consequent sluggish change in the coordination number was also recently obtained in the pressure range from 1 to 25 GPa.<sup>27</sup>

In this work, we extended the study of GeO<sub>2</sub> using EXAFS to 44 GPa and collected data over several increasing and decreasing pressure cycles. We performed a quantitative analysis for the Ge-O first shell, testing several structural models to describe the local structure. The pressure evolution of Ge-O bond lengths increased slowly and continuously up to 30 GPa suggesting that the coordination change is complete only around this pressure value.

## II. EXPERIMENT

To synthesize the GeO<sub>2</sub> glass, pure GeO<sub>2</sub> powder was fused at 1673 K for 1 h in a tube furnace and subsequently quenched. Additional details regarding the sample synthesis can be found in Ref. 28. The sample was then loaded in a symmetric diamond-anvil cell<sup>29</sup> with 400  $\mu\text{m}$  culet diamonds using a standard loading procedure without hydrostatic medium. The GeO<sub>2</sub> sample was loaded into a cubic boron nitride (BN) insert to facilitate  $I_0$  measurements (i.e., measurements could be made from within the gasket). The pressure was measured *in situ* using the ruby fluorescence technique.<sup>30</sup> X-ray absorption spectra were collected at the ID24 dispersive EXAFS beamline of European Synchrotron Radiation Facility (ESRF).<sup>31</sup> The energy-dispersive spectrometer employed a bent crystal to focus and disperse a polychromatic x-ray beam onto the sample. The beam passing through the sample then diverged toward a position-sensitive detector, in which the beam position was correlated with the energy. The x-ray beam with an energy window around the germanium  $K$  edge, was focused both in the horizontal and in the vertical planes to a  $10 \times 10 \mu\text{m}^2$  spot. The measurements were performed over compression and decompression cycles from 0 to 44 GPa.

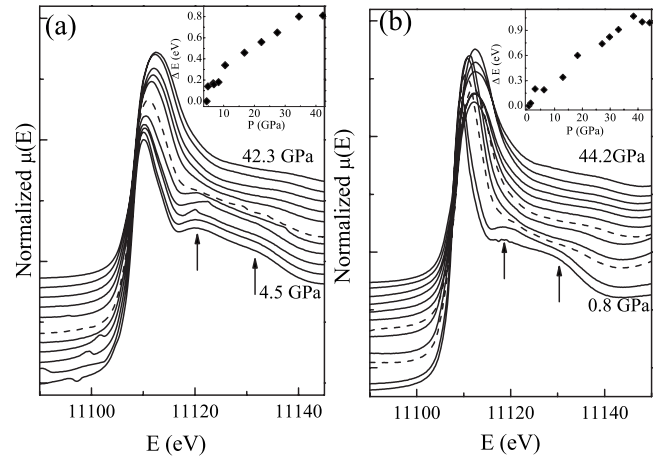


FIG. 1. Normalized XANES absorption spectra collected during (a) increasing and (b) decreasing pressure cycles. In the insets, the evolution of the edge position with respect to the lowest-pressure point is shown.

## III. EXPERIMENTAL RESULTS AND DATA ANALYSIS

Figures 1(a) and 1(b) show results from the x-ray absorption near-edge spectroscopy (XANES) region of the spectra, normalized to the jump at the absorption edge and collected upon compression and decompression cycles. Two smooth features, between 11120 and 11140 eV [see arrow in Fig. 1(a)], are observed in the spectrum collected at ambient pressure. This is in good agreement with previous x-ray absorption spectroscopy measurements for amorphous GeO<sub>2</sub>.<sup>32,33</sup> A clear modification of the main features is observed above 10 GPa [dashed spectrum in Fig. 1(a)] in the form of broadening of the white line at around 11100 eV with pressure. This is consistent with the expected coordination change and structural densification.<sup>9,32,33</sup> Similar pressure behavior is observed in the decompression cycle. However, two distinct differences can be observed in the pressure evolution of the XANES absorption spectra: the first between 13 and 18 GPa and the second between 2 and 3 GPa [shown by dashed spectra in Fig. 1(b)]. The ambient pressure spectrum collected at the end of the decompression cycle resembles the one observed at the beginning of the experiment. The evolution of the edge position with respect to the lowest-pressure point measured in both cycles (4.5 and 0.8 GPa, respectively) is shown in the two insets of Fig. 1. During both cycles, the onset of the absorption evolves continuously toward higher energies, and the energy variation is similar to the energy shift previously observed.<sup>22</sup> The EXAFS signal  $\chi(k)$ , was obtained by subtracting the embedded-atom absorption background from the measured absorption coefficient and normalizing by the edge step. The curves, multiplied by  $k$ , are shown in Fig. 2 [panels (a) and (b)] as a function of pressure. The extracted EXAFS signal was then Fourier transformed using a Hanning window in the  $k$  range of 2–8  $\text{\AA}^{-1}$ . In Fig. 2 the moduli of the Fourier transform are also shown as a function of pressure [panels (c) and (d)]. The extent of the  $k$  range in Figs. 2(a) and 2(b) is limited by the presence of Bragg reflections from the diamond anvils. The pressure behavior of the main features is consistent with

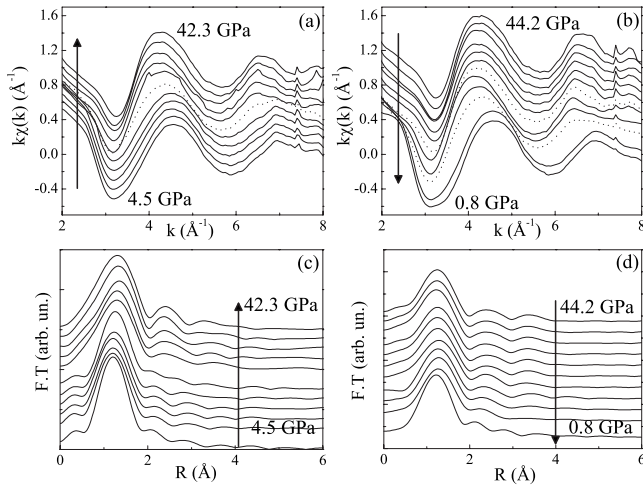


FIG. 2. Extracted  $k\chi(k)$  signals (vertically shifted) for (a) compression and (b) decompression cycles. Moduli of the Fourier transform of the experimental EXAFS spectra as the pressure (c) increases and (d) decreases.

the evolution observed in the XANES region. With increasing pressure, a shift of the EXAFS oscillations to higher  $k$  values is usually expected due to contraction of bond lengths. However, Fig. 2(a) shows that the first oscillation shifts gradually toward lower  $k$  values as the pressure is increased, and a discontinuity in the pressure evolution is clearly evident above 10 GPa [dashed spectrum in Fig. 2(a)]. This is a strong evidence in favor of a structural transformation in the sample. Similar pressure behavior is observed in the two main oscillations during the decreasing pressure cycle. In this case, two discontinuities in the pressure evolution are detected [dashed spectra in Fig. 2(b)].

The main contribution to the EXAFS signal is the single scattering between the Ge atom and the nearest oxygen atoms [the peak at 1.2 Å in Figs. 2(c) and 2(d)]. As the pressure increases, contributions from the second shell [the peak at 2.3 Å in Figs. 2(c) and 2(d)] becomes progressively more important, suggesting an enhancement of intermediate range order which is in contrast to previous results.<sup>20</sup>

#### IV. QUANTITATIVE DATA ANALYSIS

A quantitative analysis of the EXAFS signals was carried out using the ARTEMIS package.<sup>34</sup> Backscattering amplitudes and phases were calculated using the FEFF6 code for several structural models of the local structure around Ge in amorphous GeO<sub>2</sub>, based on the known crystalline phases (quartz, rutile, and monoclinic). The “quartzlike” structure locally possess four O atoms at two different distances (2+2), local structure in the rutile and in the monoclinic phases features a double (2+4) and a triple (2+2+2) Ge-O distance distribution, respectively. Since the  $k$  range of the EXAFS data is limited due to Bragg reflections from the diamond anvils [see Fig. 2 panels (a) and (b)], only one first shell Ge-O path was used to model the data. In addition, due to the strong correlation between fitting parameters, fits were performed by fixing the value of the coordination number  $N$ . The three struc-

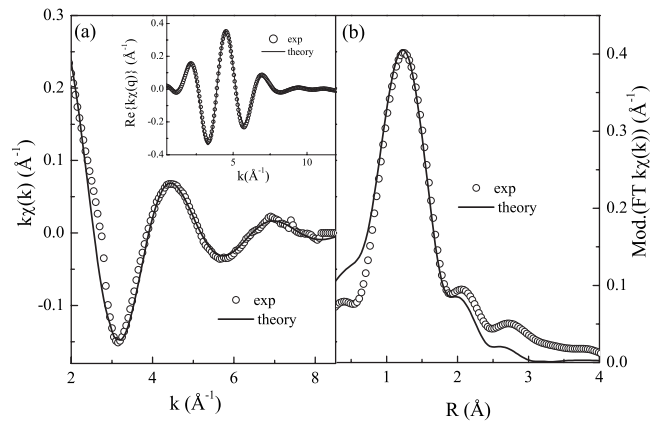


FIG. 3. Comparison between the experimental EXAFS spectrum at 8.5 GPa (shown by dots) and the best-fit calculation (shown by the solid curve) corresponding to a single-distance shell. Comparison are also reported for the extracted  $k\chi(k)$  signal [panel (a)] for the moduli of the Fourier transforms [panel (b)] and for the back-transformed signal (inset).

tural models were thus simplified to two. The first is the “fourfold coordination” model with  $N=4$  and a single average distance of  $R_{\text{quartz}}=1.72$  Å. The second one was the “sixfold coordination” model with  $N=6$  and the amplitudes and phases of the rutile or monoclinic models (we did not have the sensitivity to distinguish between the two) with average bond distances  $R_{\text{rutile}}=1.87$  Å and  $R_{\text{monoclinic}}=1.89$  Å. The “fivefold coordination” model was also tested in the fit using the Ge-O distance relative to the sixfold model and setting  $N=5$ . At the lowest pressures, the model corresponding to  $N=4$  gave the best results. Parameters for the amplitude reduction factor ( $S_0^2$ ) and the energy shift ( $E_0$ ) were fixed over the whole pressure range, using the best-fit values obtained at the lowest pressure, i.e.,  $S_0^2=0.9$  and  $E_0=5.4$  eV. The Ge-O bond distance and the mean-square relative displacement  $\sigma^2$  were left as free parameters. A comparison between the experimental spectrum collected at 8.5 GPa and the best-fit result obtained using the fourfold model is shown in Fig. 3.

The reduced  $\chi^2$  ( $\chi_v^2$ ) was used as a relevant parameter to determine which structural model best described the GeO<sub>2</sub> local structure before, during, and after the amorphous to amorphous phase transition. Three different pressure regimes can be observed by examining the evolution of  $\chi_v^2$  during the compression cycle (Fig. 4). These regimes have pressure ranges of 0–13, 13–30, and above 30 GPa, respectively. As previously mentioned, in the lowest-pressure range, the fourfold coordination model provides the best fit for describing the GeO<sub>2</sub> local structure, in good agreement with the results obtained by Itie *et al.*<sup>9</sup> In the intermediate region, the best-fit results are obtained with the fivefold-coordination model. However, the  $\chi_v^2$  values obtained with the fourfold-coordination model appear to be comparable suggesting a more complicated arrangement of the Ge-O bond lengths that deserves further attention. In the highest-pressure region the fourfold-coordination model can be definitively excluded but differences between the fivefold- and sixfold-coordination models are too small to determine whether the

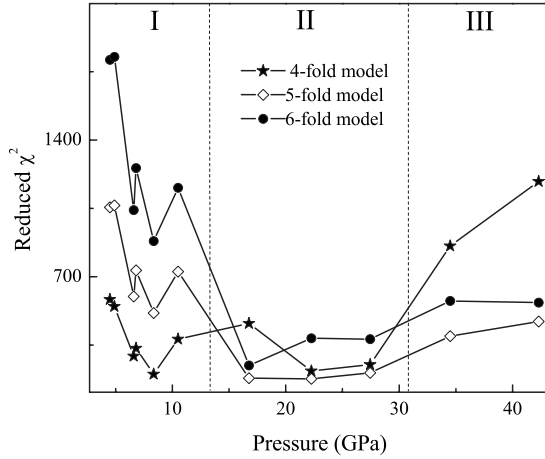


FIG. 4. Pressure behavior for the  $\chi^2_v$  obtained by analyzing the data using different structural models and coordination numbers. The dashed vertical lines indicate regions with different structures.

Ge reaches full octahedral coordination above 30 GPa. However, a clear increase in coordination number above 10 GPa can be confirmed in agreement with Itie *et al.*<sup>9</sup>

In Fig. 5, the pressure evolution of the Ge-O bond lengths and the Debye Waller factor  $\sigma^2$  are shown for both pressure cycles. Notably, the same pressure evolution was obtained for all structural models. Results obtained with  $N=6$  and  $N=5$  are both presented above 30 GPa. The Ge-O interatomic distance at ambient pressure is 1.746(7) Å, in good agreement with previous results.<sup>6</sup> A sharp increase in the Ge-O bond length is evident between 0 and 13 GPa, and is consistent with the occurrence of a phase transformation [see Fig. 5(a)]. Afterward, the bond distance increases slightly until 30 GPa where the pressure trend is clearly modified and the Ge-O distance begins to decrease. The results obtained with fivefold and sixfold models above 30 GPa are comparable within error, both leaving the pressure trend substantially unchanged. Values of  $\sigma^2$  obtained at selected pressures using

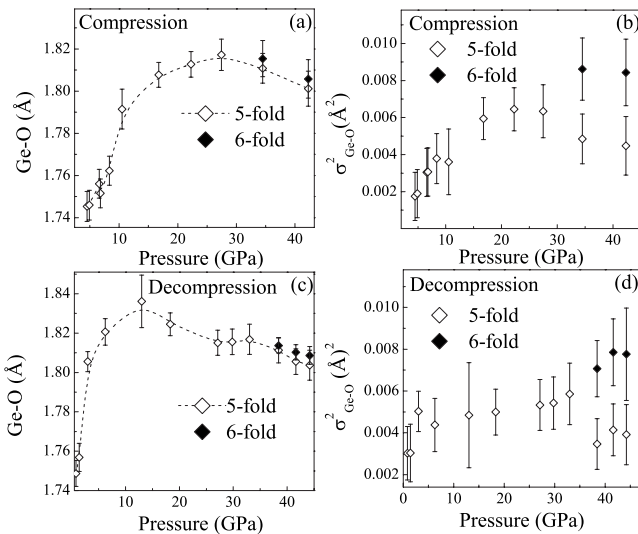


FIG. 5. Evolution of the Ge-O bond length and  $\sigma^2$  parameter during compression and decompression.

TABLE I. Values of  $\sigma^2$  obtained at selected pressures using sixfold, fivefold, and fourfold models.

Compression: $\sigma^2_{\text{Ge-O}}$ (Å <sup>2</sup> )			
$P$ (GPa)	$N=4$	$N=5$	$N=6$
4.5	0.0016(10)	0.006(2)	0.011(3)
4.9	0.0019(10)	0.006(2)	0.011(3)
16.7	0.0016(20)	0.006(1)	0.009(1)
22.3	0.0019(10)	0.006(1)	0.010(2)
34.5	0.005(2)	0.005(1)	0.009(2)
42.3	0.005(2)	0.004(1)	0.008(2)
Decompression: $\sigma^2_{\text{Ge-O}}$ (Å <sup>2</sup> )			
$P$ (GPa)	$N=4$	$N=5$	$N=6$
0.8	-0.0009(20)	0.003(1)	0.007(1)
1.4	-0.0009(30)	0.003(1)	0.007(1)
18.3	0.0006(10)	0.005(1)	0.009(1)
27.1	0.0009(10)	0.005(1)	0.009(1)
41.6	-0.0001(10)	0.004(1)	0.008(1)
44.2	-0.0005(10)	0.004(1)	0.008(1)

sixfold, fivefold, and fourfold models are reported in Table I. An increase in  $\sigma^2$  with pressure up to 10 GPa is consistent with an increase in static disorder due to the onset of the phase transition, as well as with an increase in the Ge-O bond distance driven by the coordination change [see Fig. 5(b) and Table I]. The pressure behavior of the Debye Waller parameter appears almost constant between 13 and 30 GPa. Different trends are observed above 30 GPa, depending on the coordination number that is, a further increase in the structural disorder is found if  $N=6$  or a decrease in  $\sigma^2$  is observed if  $N=5$ .

The same procedure was used to analyze the decompression cycle data. Based on the  $\chi^2_v$  values obtained by testing different structural models (not shown), the sixfold-coordination model was found to best fit the data above 30 GPa. Below 30 GPa, the fivefold model fit best. Below 13 GPa, the fourfold- and fivefold-coordination models gave similar quality fits but the former led to unphysical values for  $\sigma^2$  (see Table I). During the decompression cycle, the Ge-O interatomic distances [see Fig. 5(c)] were almost constant and comparable to the values obtained during compression in the pressure range of 44–25 GPa. Below 25 GPa, the Ge-O distances unexpectedly increased and then decreased suddenly with a different pressure evolution compared with the compression cycle. The behavior of  $\sigma^2$  is consistent with the results obtained for atomic distances [see Fig. 5(d)].

## V. DISCUSSION AND CONCLUSION

The pressure behavior of Ge-O bond lengths during compression and decompression cycles is shown in Fig. 5. We found that the pressure evolution of the Ge-O distances can

be divided into three different regions, in a manner similar to that for the reduced  $\chi^2$  as a function of pressure (see Fig. 4). A sharp increase in the Ge-O bond length was observed between 0 and 13 GPa, and this is consistent with the coordination change described in previous results.<sup>9,22</sup> In addition, no steplike evolution of the Ge-O length was observed over the 0–13 GPa pressure range, in agreement with recent results reported by Vaccari *et al.*<sup>22</sup> but in contradiction to previous results.<sup>20,21</sup> Further insights about the transition and the coordination change may be gained by considering the slight increase in the Ge-O bond distance up to 30 GPa as well as the following inversion of the pressure trend, by combining them with the pressure behavior of  $\chi_v^2$ . The evolution of  $\chi_v^2$  obtained using different structural models in the intermediate pressure range, suggests a sluggish evolution of coordination number. The coexistence of four- and five-coordinated Ge atoms in the intermediate pressure range is more reasonable than a steplike evolution with the appearance of a fully pentahedrally coordinated state. This result is supported by the evolution of the interatomic distance. Two competing mechanisms affect the evolution of Ge-O bond distances with pressure. These include the volume reduction driven by pressure which tends to decrease Ge-O lengths, and the increase in coordination number, which has the opposite effect on the atomic distances. In this scenario, the pressure trend of the bond lengths indicates that the structural transition to maximum coordination (between 5 and 6) can be considered complete only around 30 GPa.

A large hysteresis is observed in the evolution of the Ge-O distances with increasing versus decreasing pressure. The evolution of the atomic distance observed here is different for the decompression and compression cycles but is qualitatively in good agreement with previous experimental and theoretical results.<sup>9,25</sup> During decompression, an increase and a sharp decrease in Ge-O distances are observed below 25 and 10 GPa, respectively [see Fig. 5(c)]. Since two competing mechanisms affect the atomic distance evolution, the increase in the Ge-O bond lengths below 25 GPa may indicate that the volume and coordination do not follow the same path upon decompression and that the coordination change occurs at a lower pressure compared with the compression cycle. Below 3 GPa, the Ge-O bond is close to the value obtained at ambient pressure, which suggests that the coordination change is fully reversible with pressure. On the other hand, below 10 GPa reliable values of the  $\sigma^2$  parameter were only obtained using the fivefold-coordination model so a full reversibility of the coordination change cannot be claimed.

In this paper, we have extended EXAFS investigation of amorphous GeO<sub>2</sub> up to 44 GPa. The modification of local structure is continuous and gradual as the pressure increases and decreases. The local structure is well described by the fourfold-coordination structure below 10 GPa and by a structure compatible with sixfold coordination in the higher-pressure range. This is in good agreement with x-ray diffraction results obtained for crystalline sample.<sup>10,11</sup> Upon compression, a major transformation occurs, with a sharp increase in Ge-O bond lengths between 10 and 13 GPa up to values close to those expected for sixfold coordination. This is also in agreement with previous results.<sup>9</sup> We explored the

higher-pressure region, beyond 25 GPa. The sluggish increase in bond lengths observed up to 30 GPa indicates that the structural transformation is still not complete above 13 GPa. The compression of the Ge-O distances above 30 GPa seems to imply that pressure-induced densification is achieved only around this pressure value. In this scenario the coordination change appears to be more gradual and not complete at 15 GPa, in contrast with previous results.<sup>9,20,21</sup> This confirms the most recent EXAFS results between 0 and 13 GPa obtained by Vaccari *et al.*<sup>22</sup> The pressure evolution of the  $R\chi^2$  parameter reveals a mixed state in which four- and five-coordinated Ge atoms coexist in the wide pressure range between 13 and 30 GPa. This is in good agreement with theoretical calculations performed by Shanavas *et al.*,<sup>25</sup> by Micoulaut *et al.*,<sup>24,26</sup> and by Li *et al.*<sup>27</sup> in which the number of oxygen atoms around a Ge atom slowly reaches the octahedral limit and the state is still not fully sixfold coordinated, even at 30 GPa. Although the analysis of our data indicates that both  $N=5$  and  $N=6$  coordination are equally probable above 30 GPa, the combination of our results with previous work suggests that the achievement of a fully sixfold densified state is possible in amorphous GeO<sub>2</sub> only above 30 GPa. Upon decompression the Ge-O bond-length evolution is in good agreement with the results of Refs. 9 and 25. On the other hand, the presence of five-coordinated Ge atoms cannot be ruled out at ambient pressure, and the complete reversibility of the coordination change cannot be ascertained.

In conclusion the present measurements provide the first EXAFS characterization of amorphous GeO<sub>2</sub> up to 44 GPa. In contrast with previous experimental results, our results show that the transformation in coordination number occurs gradually and can be considered complete only above 30 GPa. Therefore, the high-pressure behavior of amorphous GeO<sub>2</sub> is qualitatively similar to that observed in amorphous SiO<sub>2</sub>, although their crystalline counterparts display quite distinct high-pressure behaviors. Indeed, unlike crystalline GeO<sub>2</sub> for which the pressure-induced structural transformations are quite well established,<sup>6</sup> the reported high-pressure behavior of  $\alpha$ -quartz SiO<sub>2</sub> is particularly complex and still a matter of debate. It appears to be strictly correlated with hydrostatic conditions.<sup>35,36</sup> Crystalline SiO<sub>2</sub> has been made amorphous between 25 and 35 GPa.<sup>36</sup> An unknown quartz II high-pressure phase was detected in quasihydrostatic conditions above 16 GPa, and increasing the pressure to 25 GPa resulted in new diffraction peaks corresponding to poorly crystalline monoclinic  $P2_1/c$  structure.<sup>35</sup> In contrast to the crystalline phase, but similar to the amorphous GeO<sub>2</sub>, a slow transformation from a fourfold to a sixfold coordinate structure is observed in SiO<sub>2</sub> glass although the transformation process occurs at higher-pressure values. SiO<sub>2</sub> glass behaves as a single amorphous polymorph having a fourfold-coordinated structure up to 10 GPa. Irreversible changes in the short-range order begin at approximately 25 GPa and the coordination number continuously increases from four to six with increasing pressure up to 40–45 GPa where the amorphous SiO<sub>2</sub> behaves as a single amorphous polymorph having a sixfold-coordinated structure.<sup>37–39</sup>

The present measurements show the appearance of a state in which different Ge coordinations are present over a wide pressure range, from 13 to 30 GPa. The validity of both the

fourfold and the fivefold models over the entire intermediate pressure range indicates that this state may be more accurately identified as a simple mixture of four- and five-coordinated germanium-centered polyhedra rather than a new intermediate state with a stable fivefold unit, as suggested in Refs. 20 and 21. Finally, the present results shed light on the GeO<sub>2</sub> densification process and on the nature of the amorphous-amorphous transition. Although a definite understanding of the nature of the amorphous transition can be drawn from only knowing the pressure evolution of the GeO<sub>2</sub> volume, the gradual increase in the Ge-O bond distances up to 30 GPa and the appearance of a disordered state in the intermediate pressure range suggest that the amorphous-amorphous transition is gradual and continuous

rather than abrupt, as would be expected in the case of a first-order transition.

#### ACKNOWLEDGMENTS

This work is supported by the Department of Energy, Office of Basic Sciences, Division of Material Science and Engineering under Contract No. DE-AC02-76SF00515. We also wish to thank K. V. Shanavas for fruitful discussions. Part of this work is also supported by EFree, and Energy Frontier Research Center funded by U.S. Department of Energy, Office of Science, Office of Basic Energy Sciences under Grant No. DE-SC0001057.

\*Corresponding author; baldini@stanford.edu

- <sup>1</sup>P. J. Heaney, *Silica: Physical Behavior, Geochemistry and Materials Applications* (Mineralogical Society of America, Washington, DC, 1994).
- <sup>2</sup>M. C. Wilding, M. Wilson, and P. F. McMillan, *Chem. Soc. Rev.* **35**, 964 (2006).
- <sup>3</sup>V. V. Brazhkin and A. G. Lyapin, *J. Phys.: Condens. Matter* **15**, 6059 (2003).
- <sup>4</sup>P. F. McMillan, *J. Mater. Chem.* **14**, 1506 (2004).
- <sup>5</sup>P. F. McMillan, M. Wilson, M. C. Wilding, D. Daisenberger, M. Mezouar, and G. N. Greaves, *J. Phys.: Condens. Matter* **19**, 415101 (2007).
- <sup>6</sup>M. Micoulaut, L. Cormier, and G. S. Henderson, *J. Phys.: Condens. Matter* **18**, R753 (2006).
- <sup>7</sup>G. S. Smith and P. B. Isaacs, *Acta Crystallogr.* **17**, 842 (1964).
- <sup>8</sup>W. H. Baur and A. A. Khan, *Acta Crystallogr., Sect. B: Struct. Crystallogr. Cryst. Chem.* **27**, 2133 (1971).
- <sup>9</sup>J. P. Itie, A. Polian, G. Calas, J. Petiau, A. Fontaine, and H. Tolentino, *Phys. Rev. Lett.* **63**, 398 (1989).
- <sup>10</sup>J. Haines, J. M. Leger, and C. Chateau, *Phys. Rev. B* **61**, 8701 (2000).
- <sup>11</sup>V. P. Prakapenka, G. Shen, L. S. Dubrovinsky, M. L. Rivers, and S. R. Sutton, *J. Phys. Chem. Solids* **65**, 1537 (2004).
- <sup>12</sup>V. V. Brazhkin, E. V. Tat'yanin, A. G. Lyapin, S. V. Popova, O. B. Tsiok, and D. V. Balitski, *JETP Lett.* **71**, 293 (2000).
- <sup>13</sup>J. Haines, J. M. Leger, C. Chateau, and A. S. Pierera, *Phys. Chem. Miner.* **27**, 575 (2000).
- <sup>14</sup>S. Ono, K. Hirose, N. Nishiyama, and M. Isshiki, *Am. Mineral.* **87**, 99 (2002).
- <sup>15</sup>S. Ono, T. Tsuchiya, K. Hirose, and Y. Ohishi, *Phys. Rev. B* **68**, 014103 (2003).
- <sup>16</sup>G. H. Wolf, S. Wang, C. A. Herbst, D. J. Durban, W. F. Oliver, Z. C. Zang, and K. Halvorson, in *High-Pressure Research: Application to Earth and Planetary Sciences*, edited by Y. Syono and M. H. Manghnani (Terra Scientific, Tokyo/American Geophysical Union, Washington, DC, 1992), p. 503.
- <sup>17</sup>P. S. Salmon, A. C. Barnes, R. A. Martin, and G. J. Cuello, *Phys. Rev. Lett.* **96**, 235502 (2006).
- <sup>18</sup>C. H. Polsky, K. H. Smith, and G. H. Wolf, *J. Non-Cryst. Solids* **248**, 159 (1999).
- <sup>19</sup>K. H. Smith, E. Shero, A. Chizmeshya and G. H. Wolf, *J. Chem. Phys.* **102**, 6851 (1995).
- <sup>20</sup>M. Guthrie, C. A. Tulk, C. J. Benmore, J. Xu, J. L. Yarger, D. D. Klug, J. S. Tse, H-k. Mao, and R. J. Hemley, *Phys. Rev. Lett.* **93**, 115502 (2004).
- <sup>21</sup>X. Hong, G. Shen, V. B. Prakapenka, M. Newville, M. L. Rivers, and S. R. Sutton, *Phys. Rev. B* **75**, 104201 (2007).
- <sup>22</sup>M. Vaccari, G. Aquilanti, S. Pascarelli, and O. Mathon, *J. Phys.: Condens. Matter* **21**, 145403 (2009).
- <sup>23</sup>G. Shen, H. Liermann, S. Sinogeikin, W. Yang, X. Hong, C.-S. Yoo, and H. Cynn, *Proc. Natl. Acad. Sci. U.S.A.* **104**, 14576 (2007).
- <sup>24</sup>M. Micoulaut, *J. Phys.: Condens. Matter* **16**, L131 (2004).
- <sup>25</sup>K. V. Shanavas, N. Garg, and S. M. Sharma, *Phys. Rev. B* **73**, 094120 (2006).
- <sup>26</sup>M. Micoulaut, Y. Guissani, and B. Guillot, *Phys. Rev. E* **73**, 031504 (2006).
- <sup>27</sup>T. Li, S. Huang, and J. Zhu, *Chem. Phys. Lett.* **471**, 253 (2009).
- <sup>28</sup>Sung Keun Lee and Bum Han Lee, *J. Phys. Chem. B* **110**, 16408 (2006).
- <sup>29</sup>H-k. Mao and P. M. Bell, *Design and Varieties of the Megabar Cell* (Carnegie Institute of Washington, Washington, 1978), Vol. 77, pp. 904–908.
- <sup>30</sup>H-k. Mao, J. Xu, and P. M. Bell, *J. Geophys. Res.* **91**, 4673 (1986).
- <sup>31</sup>S. Pascarelli, O. Mathon, and G. Aquilanti, *J. Alloys Compd.* **362**, 33 (2004).
- <sup>32</sup>O. Ohtaka, A. Yoshiasa, H. Fukui, K. Murai, M. Okube, H. Takebe, Y. Katayama, and W. Utsumi, *J. Phys.: Condens. Matter* **14**, 10521 (2002).
- <sup>33</sup>L. Cormier, G. Ferlat, J.-P. Itie, L. Galois, G. Calas, and G. Aquilanti, *Phys. Rev. B* **76**, 134204 (2007).
- <sup>34</sup>J. J. Rehr and R. C. Albers, *Rev. Mod. Phys.* **72**, 621 (2000); B. Ravel and M. Newville, *J. Synchrotron Radiat.* **12**, 537 (2005).
- <sup>35</sup>J. Haines, J. M. Leger, F. Gorelli, and M. Hanfland, *Phys. Rev. Lett.* **87**, 155503 (2001).
- <sup>36</sup>R. H. Hemley, A. P. Jephcoat, H-k. Mao, L. C. Ming, and M. H. Manghnani, *Nature (London)* **334**, 52 (1988).
- <sup>37</sup>T. Sato and N. Funamori, *Phys. Rev. Lett.* **101**, 255502 (2008).
- <sup>38</sup>Y. Inamura, Y. Katayama, W. Utsumi, and K. I. Funakoshi, *Phys. Rev. Lett.* **93**, 015501 (2004).
- <sup>39</sup>C. Meade, R. J. Hemley, and H-k. Mao, *Phys. Rev. Lett.* **69**, 1387 (1992).